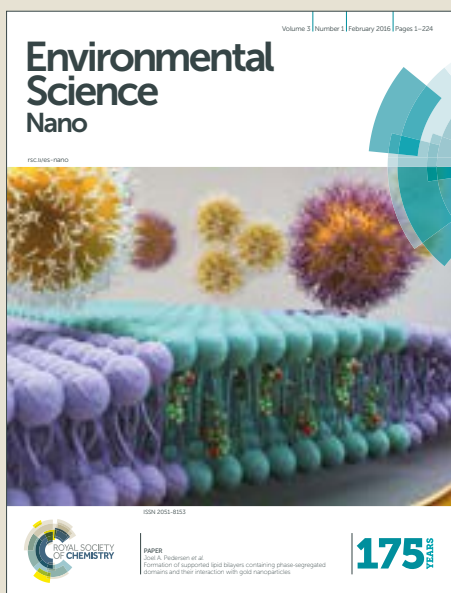


# Environmental Science Nano

Accepted Manuscript



This article can be cited before page numbers have been issued, to do this please use: C. Della Torre, M. Parolini, L. Del Giacco, A. Ghilardi, M. Ascagni, N. Santo, D. Maggioni, S. Magni, L. Madaschi, L. Prospero, C. A. M. La Porta and A. Binelli, *Environ. Sci.: Nano*, 2017, DOI: 10.1039/C7EN00154A.



This is an Accepted Manuscript, which has been through the Royal Society of Chemistry peer review process and has been accepted for publication.

Accepted Manuscripts are published online shortly after acceptance, before technical editing, formatting and proof reading. Using this free service, authors can make their results available to the community, in citable form, before we publish the edited article. We will replace this Accepted Manuscript with the edited and formatted Advance Article as soon as it is available.

You can find more information about Accepted Manuscripts in the [author guidelines](#).

Please note that technical editing may introduce minor changes to the text and/or graphics, which may alter content. The journal's standard [Terms & Conditions](#) and the ethical guidelines, outlined in our [author and reviewer resource centre](#), still apply. In no event shall the Royal Society of Chemistry be held responsible for any errors or omissions in this Accepted Manuscript or any consequences arising from the use of any information it contains.

Environmental significance statement

The toxicity and bioavailability of pollutants could be enhanced by their interaction with nanomaterials. This new aspect could lead to unpredictable impacts for aquatic wildlife. We studied the possible carrier role of carbon nanopowder for benzo( $\alpha$ )pyrene on zebrafish embryos. Our results clearly show that the adsorption to nanopowder modifies the uptake and the distribution of the pollutant in the organism. The benzo( $\alpha$ )pyrene bound to nanopowder is able to interfere with important cellular targets in a different way in comparison to the pollutant alone. This study opens new views of nano-ecotoxicity highlighting the importance of the interaction between nanomaterials and environmental pollutants. Moreover, our study provides a new methodologic strategy to investigate their effects *in vivo*.

Environmental Science: Nano Accepted Manuscript

1  
2  
3  
4  
5  
6  
7  
8  
9  
10  
11  
12  
13  
14  
15  
16  
17  
18  
19  
20  
21  
22  
23  
24  
25  
26  
27  
28  
29  
30  
31  
32  
33  
34  
35  
36  
37  
38  
39  
40  
41  
42  
43  
44  
45  
46  
47  
48  
49  
50  
51  
52  
53  
54  
55  
56  
57  
58  
59  
60

## Adsorption of B( $\alpha$ )P on Carbon Nanopowder affects accumulation and toxicity on zebrafish (*Danio rerio*) embryos

Camilla Della Torre<sup>1\*</sup>, Marco Parolini<sup>1</sup>, Luca Del Giacco<sup>1</sup>, Anna Ghilardi<sup>1</sup>, Miriam Ascagni<sup>1</sup>, Nadia Santo<sup>1</sup>, Daniela Maggioni<sup>2</sup>, Stefano Magni<sup>1</sup>, Laura Madaschi<sup>1</sup>, Laura Prospero<sup>1</sup>, Caterina La Porta<sup>1,3</sup>, Andrea Binelli<sup>1\*</sup>

<sup>1</sup>Department of Biosciences, University of Milan, Via Celoria 26, 20133 Milan, Italy

<sup>2</sup>Department of Chemistry, University of Milan Via Golgi 19, 20133 Milan, Italy

<sup>3</sup>Centre for Complexity & Biosystems, University of Milan, Via Celoria 26, 20133 Milan, Italy

\*corresponding authors

The increasing use of nanomaterials opens several concerns regarding their potential risk for the environment and human health. In particular, the aquatic ecosystems appear highly susceptible. Our research wanted to breakthrough this aspect investigating the interplay between carbon nanopowder (CNPW) and a common pollutant such as Benzo( $\alpha$ )pyrene (B( $\alpha$ )P) in zebrafish embryos. To this aim CNPW was contaminated with B( $\alpha$ )P, showing significant adsorption properties towards the hydrocarbon. Embryos were then exposed to CNPW (50 mg/L), B( $\alpha$ )P (0.2-6-20  $\mu$ g/L) alone and to the CNPW doped with the three B( $\alpha$ )P concentrations. We demonstrated that CNPW helps B( $\alpha$ )P uptake by zebrafish embryos and we also demonstrated that the interaction between CNPW and the hydrocarbon affects the organism stress response pathways eliciting their toxic effect. In particular, the modulation of genes related to the cellular stress response (*cyp1a*, *hsp70*, *sod1*, *sod2*) and the measure of oxidative stress enzyme activities allowed us to identify critical molecular events, modulated by the pollutants alone and in co-exposure. Finally, to evaluate the toxic effects due to CNPW interaction with B( $\alpha$ )P, we analyzed biomarkers of cyto/genotoxicity. As far as no significant genotoxicity was induced by B( $\alpha$ )P and CNPW alone, the co-exposure led to an increase of cytotoxicity, and higher incidence of necrotic and apoptotic cells. Altogether our data show that nanomaterials, even if they are not toxic *per se*, could help common pollutants to enhance their toxicity.

## Introduction

Nanoscale science and technology are providing unprecedented and revolutionary advances in several technology and industry sectors. While benefits and improvements of nanotechnology are well established, several concerns have raised regarding the potential risk of nanomaterials (NMs) for the environment and human health.<sup>1,2</sup> The aquatic ecosystems in particular are highly susceptible to such contamination, being the sink of NMs released from soil, wastewaters and aerial depositions, as well as from direct applications.<sup>3</sup> Several studies on aquatic organisms have provided data which highlight the harmful effects of NMs.<sup>4-6</sup> Carbon-based NMs (CNMs) in particular have the ability to impact biological systems due to their physico-chemical properties and biological reactivity.<sup>7</sup> Besides acute toxicity, several sub-lethal effects as genotoxicity, cytotoxicity, oxidative injuries, inflammation, behavioural alterations and reproduction impairment have been documented in aquatic models.<sup>8-13</sup>

Another extremely important feature of NMs is the ability to interact with many environmental pollutants, such as metals and man-made chemicals. The interactive effects of either metal and carbon-based nanoparticles (NPs) with different environmental pollutants have been extensively investigated on aquatic organisms.<sup>14-21</sup> As for carbon-based NPs (fullerenes and nanotubes), most of the studies showed a high sorption capacity towards hydrophobic chemicals.<sup>22-25</sup> Nevertheless the ecotoxicological consequences of such interactions for natural aquatic environment are hardly predictable, as the studies undertaken so far provide inconsistent results. In some cases it is highlighted the ability of NPs to adsorb and sequester the contaminants, thereby reducing their bioavailability for organisms.<sup>26,27</sup> On the contrary, other studies indicate that the adsorption of pollutants on NPs might increase their cellular uptake and accumulation.<sup>28-29</sup>

Such uncertainties call the need for a deep understanding of complex mechanisms that occur once CNMs and pollutants meet each other, starting from a thorough evaluation of chemico-physical interactions and how these interactions affect pollutants uptake and distribution inside the biological system and affect cellular pathways leading to toxicity. Therefore, this study was aimed at evaluating the interactions between Carbon Nanopowder (CNPW) -representative of carbon nanoparticulate amorphous form- and the carcinogen Benzo( $\alpha$ )pyrene (B( $\alpha$ )P) on zebrafish (*D. rerio*) embryos. We doped CNPW with three different concentrations of B( $\alpha$ )P, whose sorption on CNPW has been measured by gas chromatography-mass spectrometry (GC-MS/MS) and exposed zebrafish embryos to single contaminants administered alone (CNPW; B( $\alpha$ )P) or in co-exposure (CNPW+ B( $\alpha$ )P). The novelty of our experimental is to assess the accumulation and biological effects only of the B( $\alpha$ )P bound to CNPW without any interference of free hydrocarbon. A suite of biomarkers was also applied based on the postulated mechanisms of toxicity described for CNMs which involved the generation of oxidative stress<sup>30</sup> and DNA damage.<sup>31</sup> The expression of genes related to cell stress response such as *cyp1a*, *sod1*, *sod2* and *hsp70* and the activity of proteins involved in the antioxidant response machinery as glutathione-S-transferase (GST), catalase (CAT) and superoxide dismutase (SOD) were measured, to evaluate whether the combination of B( $\alpha$ )P with CNPW induces different molecular pathways respect to the pollutants alone. Finally, the cyto-genotoxicity of the pollutants alone and in combination was compared by the application of trypan blue exclusion method,

single gel cell electrophoresis, DNA diffusion assay and Micronucleus test, confirming the enhancing effect of the CNPW on the pollutant toxicity.

## Methods

### *Chemicals and reagents*

The CBNW was purchased by Sigma-Aldrich (CAS n. 7440-44-0). The advertised particle size was <50 nm (TEM) and the specific surface area >100 m<sup>2</sup>/g (BET). Bulk powder was observed by scanning electron microscopy (SEM Zeiss LEO 1430). The powder was mounted onto an aluminium stub and gold coated.

B( $\alpha$ )P powder and PAHs' standard (PAH-Mix 14) were supplied by Dr. Ehrenstorfer. All solvents used for PAHs' determination were pesticide grade from Sigma-Aldrich. Reagents for biomarkers and immunostaining were purchased from Sigma-Aldrich. Reagents for RNA extraction and quantitative RT-PCR were from Promega and Biorad.

### *CNPW clean-up and characterization*

An aliquot (5 g) of CNPW standard was cleaned-up with toluene in a Soxhlet apparatus (FALC Instruments, Lurano, Italy) up to 92 h. One hundred mL of toluene were collected after 24-48-52-90 h to monitor the clean-up process over time. We added 20 mL of isooctane to the samples, which were then concentrated to a volume of 1 mL using a rotary evaporator (RV 06-LR, IKA, Staufen, Germany) followed by a gentle nitrogen flow. The effective elimination of PAHs' impurities over time was evaluated by GC-MS/MS.

Purified CNPW was resuspended in milliQ water, stirred for 48 h and sonicated for 15 min and observed through transmission electron microscopy (TEM) for size and shape determination. A drop of CNPW dispersion was placed on 300 mesh formvar copper grids and the excess of water was gently blotted using filter paper. Images were acquired using a Zeiss LEO 912ab Energy Filtering TEM operating at 100 kV, at a magnification of 25-50,000 using a CCD-BM/1 K system. Size distribution of the CNPW suspended in water and surface charge ( $\zeta$  potentials) were determined by Dynamic Light Scattering (DLS) at 298 K, by using a Malvern Zetasizer nano ZS instrument (Malvern instruments, UK), equipped with solid state He-Ne laser operating at a wavelength of 633 nm and detecting the scattered light at a scattering angle of 173°. Data were elaborated through the Zetasizer Nano Series software, version 7.02 (Particular Sciences, UK).

### *B( $\alpha$ )P adsorption*

Three suspensions of purified CNPW were prepared by dispersing it in milliQ water at 1 g/L and by sonication (15 min) with a probe sonicator (ST.IM.IN Milan) at 12,000 Hz. Proper volumes of B( $\alpha$ )P dissolved in dimethylsulphoxide (DMSO) were added to reach the nominal concentrations of 1, 0.1 and 0.01 mg/L. The suspensions were then stirred for 72 h at 20 °C. At the end of the adsorption process, each suspension was centrifuged for 15 min at 3,000 x g. The CNPW pellets were dried in an oven for 24 h. An aliquot of about 70 mg of each contaminated CNPW was extracted with toluene in a Soxhlet extractor for 24 h and the B( $\alpha$ )P effective adsorption on CNPW was measured by GC-MS/MS.

### *GC-MS/MS analysis of PAHs*

An aliquot of 2  $\mu\text{L}$  was injected into a GC chromatograph (TRACE GC, Thermo-Electron, Texas, USA) equipped with a programmed temperature vaporizer (PTV) injector, an AS 2000 autosampler (Thermo Electron) and an Rtx-5MS (Restek, Bellefonte, PA, USA) capillary column (30 m length, 0.25 mm I.D., 0.25  $\mu\text{m}$  film thickness). The gas chromatograph was coupled with a PolarisQ Ion Trap mass spectrometer. Chromatographic conditions were as follows: PTV in solvent split mode (split flow= 50  $\text{mL min}^{-1}$ ) and splitless time of 2 min; carrier gas helium at 1.2  $\text{mL min}^{-1}$ ; surge pressure of 280 kPa; injection pressure of 67 kPa; transfer pressure of 134 kPa; injector temperature starting at 70  $^{\circ}\text{C}$  and held for 1.2 min, then ramped to 300  $^{\circ}\text{C}$  at 14  $^{\circ}\text{C s}^{-1}$  and held for 1.2 min; oven temperature starting at 70  $^{\circ}\text{C}$  and held for 1.2 min, then ramped to 220  $^{\circ}\text{C}$  at 40  $^{\circ}\text{C min}^{-1}$  and held for 1 min, and finally ramped to 290  $^{\circ}\text{C}$  at 4  $^{\circ}\text{C min}^{-1}$  and held for 8 min. PAHs were quantified by GC/MS under the following instrumental conditions: Selective Ion Monitoring (SIM) mode after Electron Ionization (EI) with standard electron energy of 70 eV; transfer line at 280  $^{\circ}\text{C}$ ; ion source at 260  $^{\circ}\text{C}$  and the damping gas at 1  $\text{mL min}^{-1}$ . Quantitative analyses were performed using Excalibur software (Thermo Electron) with external calibration curves ranging from 10 to 50  $\mu\text{g/L}$ . A blank sample was run in parallel. The most volatile PAHs, showing non-negligible concentrations, were corrected by the blanks.

### *Preparation of CNPW suspensions and hydrodynamic behaviour in exposure media*

Suspensions of purified CNPW and CNPW contaminated with B( $\alpha$ )P at concentration of 50  $\text{mg/L}$  were equilibrated in zebrafish water (ZFW) for one week by stirring in the dark at 20  $^{\circ}\text{C}$ . Hydrodynamic diameters and surface charges ( $\zeta$  potentials) of all samples were determined by DLS as described above. Time-dependent variations of the size distributions of the CNPW suspensions in zebrafish water were also monitored, at 2-4-24 h recording each measurement in quadruplicate.

### *Zebrafish embryos exposure*

Zebrafish embryos of the AB strain were obtained from adult fish reared in the zebrafish facility of the Department of Bioscience, University of Milan. Our facility strictly complies with the relevant Italian laws, rules and regulations (Legislative Decree No. 116/92), as confirmed by the authorization issued by the municipality of Milan (Art. 10 of Legislative Decree No. 116, dated 27.1.1992). The whole procedure was carried out in accordance with the relevant guidelines and regulations.

To avoid any physical interference with the uptake of CNPW, the chorion was removed by enzymatic reaction with pronase (0.5  $\text{mg/mL}$ ) at 24 hours post-fertilization (hpf), immediately prior to the exposure. Dechorionated embryos were exposed in Petri dishes (4 mL) to B( $\alpha$ )P alone (0.2, 6, 20  $\mu\text{g/L}$ ), CNPW (50  $\text{mg/L}$ ) alone and contaminated with B( $\alpha$ )P (CNPW + B( $\alpha$ )P 0.2  $\mu\text{g/L}$ , CNPW + B( $\alpha$ )P 6  $\mu\text{g/L}$ , CNPW + B( $\alpha$ )P 20  $\mu\text{g/L}$ ). B( $\alpha$ )P concentrations were defined based on the effective B( $\alpha$ )P sorption on CNPW (50  $\text{mg/L}$ ) measured at GC-MS/MS (see results, Tab. 2). Control animals were exposed to zebrafish water (ZFW) and to vehicle (0.1% DMSO) only.

1  
2  
3  
4  
5  
6  
7  
8  
9  
10  
11  
12  
13  
14  
15  
16  
17  
18  
19  
20  
21  
22  
23  
24  
25  
26  
27  
28  
29  
30  
31  
32  
33  
34  
35  
36  
37  
38  
39  
40  
41  
42  
43  
44  
45  
46  
47  
48  
49  
50  
51  
52  
53  
54  
55  
56  
57  
58  
59  
60

Based on several preliminary range-finding experiments, the adopted CNPW and B( $\alpha$ )P concentrations did not produce mortality or teratogenic effects. Anyhow, these endpoints were checked at the end of each exposure experiment.

The exposure proceeded until 96 hpf under semistatic conditions, and the exposure solutions were changed every 24 h. For gene expression and biochemical analyses each batch of treated and control embryos was placed in 1.5 mL microtubes and stored at -80 °C until processing. For genotoxicity assessment, embryos were processed immediately at the end of the exposure as described below. A companion exposure aimed at assessing the uptake/accumulation of CNPW and B( $\alpha$ )P was performed exposing embryos in ZFW containing 0.003% 1-phenyl 2-thiourea (PTU) to prevent pigmentation. At the end of exposures, embryos were fixed in paraformaldehyde (4% in 0.1 M phosphate buffered solution at pH 7.2 - PB). With the aim to accurately localize B( $\alpha$ )P fluorescence signal inside embryos, we used the *fli1:GFP* transgenic line *Tg(fli1a:EGFP)*,<sup>32</sup> which enables the visualization of the circulatory system in green. Experiments were run at least 3 times for each analysis.

### ***Whole mount confocal microscopy***

To define the B( $\alpha$ )P uptake localization in embryos, we recorded the B( $\alpha$ )P fluorescence signal through confocal microscopy. This technique has been recognized as reliable indicator of hydrocarbon exposure in biological systems including fish embryos.<sup>33,34</sup> Z-stacks of whole mount *Tg(fli1a:EGFP)* zebrafish embryos were collected using a Leica SP2 laser scanning confocal microscope (Leica Microsystems) with a Plan-Apochromat 10x/0.4 objective. To record the B( $\alpha$ )P-associated fluorescence, images were acquired using 405 nm excitation laser and the emission signal was collected in the range of 410-550nm. The maximum projection of fluorescence images was achieved for each embryo (n = 3) and was analyzed using ImageJ analysis software v.1.49k. To quantify B( $\alpha$ )P accumulation, the Integrated Density (Area x Mean Grey Level) was calculated.

### ***CNPW localization***

For CNPW localization embryos were cryoprotected in sucrose 15 % for 2h and sucrose 30 % overnight a 4 °C. Sections (10 $\mu$ m) were cut by a cryostat (Leica CM1850) and were sequentially incubated in 0.05 M NH<sub>4</sub>Cl in PB for 30 min to quench free aldehyde groups, in 0.01 M phosphate-buffered saline pH 7.4 (PBS) containing 1% bovine serum albumin (BSA) and 0.2 % Triton X-100 (30 min). Sections were exposed to phalloidin (Cytoskeleton 555 actin stain, TRITC conjugate, PHDH1) which binds with the filamentous actin, for 2 h at room temperature, washed extensively in PBS and mounted in PBS/glycerol (1:2 v/v), with DNA-binding dye 4'-6-diamidino-2-phenylindole (DAPI –specific fluorescent probe). Sections were observed with confocal microscope Leica SP2 microscope with He/Kr and Ar lasers (Leica, Wetzlar, Germany) and CNPW was visualized in reflection mode at 488 nm. For the localization of nanoscale CNPW by ultrastructural analysis, 10 embryos from each experimental group were fixed in a mixture of 4% paraformaldehyde and 2.5% glutaraldehyde in 0.1 M sodium cacodylate buffered solution at pH 7.4. After washes in the same

1  
2  
3  
4  
5  
6  
7  
8  
9  
10  
11  
12  
13  
14  
15  
16  
17  
18  
19  
20  
21  
22  
23  
24  
25  
26  
27  
28  
29  
30  
31  
32  
33  
34  
35  
36  
37  
38  
39  
40  
41  
42  
43  
44  
45  
46  
47  
48  
49  
50  
51  
52  
53  
54  
55  
56  
57  
58  
59  
60

buffer, embryos were postfixed in 1% OsO<sub>4</sub>, dehydrated in a graded ethanol series and infiltrated in Araldite-Epon. Sectioning was performed using an Ultracut E microtome (Reichert, Austria). Ultrathin sections of about 70 nm were collected on 600-mesh uncoated copper grids. Sections were not counterstained to avoid interference with CNPW visualization. Digital images were acquired using a CCD-BM/1K system, and image elaboration was performed using the ESI vision software AnalySIS (Soft Imaging Systems, Muenster, Germany). The identity of CNPW was confirmed through Electron Spectroscopy Imaging, using a Zeiss LEO 912ab energy-filtering transmission electron microscope.

### ***RNA extraction and quantitative RT-PCR (qRT-PCR)***

Total RNA was isolated using SV Total RNA Isolation System (Promega, Madison, Wisconsin). Each sample was incubated with DNase to eliminate any genomic DNA residue from the RNA preparation. First-strand cDNAs were synthesized employing the ImProm-II Reverse Transcription System (Promega), according to the manufacturer's protocol, using random oligonucleotides to prime the reverse transcription of 1 µg of total RNA. qPCRs were performed using *cyp1a*, *hsp70*, *sod1* and *sod2* specific primers (see table S1 for sequences). For normalization purposes, 18S ribosomal RNA level was also tested in all the samples. Reactions were performed in a 96-well format iQ5<sup>TM</sup> Multicolor Real-Time PCR Detection System (Biorad) using the iQ<sup>TM</sup> SYBR® Green Supermix (Biorad). Three independent qRT-PCR experiments from the same reverse transcribed sample were performed using a pair of gene-specific primers. The presence of a single PCR product was verified by melting-curve and agarose gel analyses. The gene expression levels were considered significantly different when 2-fold higher or lower than those measured in controls (0.5 < not significant <2).

### ***Biochemical analysis***

Pools of 60 embryos were homogenized using a pestle in 100 mM potassium phosphate buffer (KCl 100 mM, EDTA 1 mM, protease inhibitors 1:100 v/v, dithiothreitol 1 mM pH 7.4). The homogenates were centrifuged at 15,000 x g for 10 min at 4 °C. The supernatant was collected and GST, SOD and CAT activities were immediately measured in triplicate. The GST activity was measured by adding reduced glutathione (1 mM) in 100 mM phosphate buffer (pH 7.4) and using CDNB (1mM) as substrate. The reaction was monitored for 1 min at 340 nm. The CAT activity was determined by measuring the consumption of H<sub>2</sub>O<sub>2</sub> (50 mM) in 100 mM potassium phosphate buffer (pH 7) at 240 nm. The SOD activity was determined by measuring the degree of inhibition of cytochrome c (10 µM) reduction by the superoxide anion generated by the xanthine oxidase (1.87 mU/mL)/hypoxanthine (50 µM) reaction at 550 nm. The activity is given as SOD units (1 SOD unit=50% inhibition of the xanthine oxidase reaction).

The total protein content of each sample was measured according to the Bradford (1976)<sup>35</sup> method using bovine serum albumin as standard.



### **Genotoxicity**

Biomarkers of cyto-genotoxicity were performed on cells dissociated from a pool of ten zebrafish embryos (three pools per treatment). Since biomarker methods are described elsewhere,<sup>36</sup> a brief description was reported here. Cell viability was assessed by the trypan blue dye exclusion method. Embryo cell suspension (10  $\mu$ L) was mixed with 10  $\mu$ L of 0.4 % (w/v) trypan blue solution in PBS and transferred to a hemocytometer. Non-viable cells were stained deep blue, whereas viable cells were colorless. Three replicates per experimental group were performed. The alkaline (pH > 13) Single Cell Gel Electrophoresis (SCGE) assay was performed according to the method described in Koshmel et al. (2008).<sup>37</sup> One hundred cells per slide (n = 9; three slides per each pool) were analyzed using the Comet Score<sup>®</sup> image analysis software. The percentage of DNA in the comet tail was used as endpoints of primary genetic injuries. The apoptotic cell frequency (%) was assessed<sup>38</sup> analyzing three hundreds cells per slide (n=6; two slides per each pool). The frequency of micronuclei (MN%) was calculated on 400 cells/slide (n=6; two slides per each pool) according to Pavlica et al. (2000).<sup>39</sup>

### **Statistical analysis**

To evaluate differences between control and treated groups the one-way analysis of variance (ANOVA) was applied to data from biomarker and fluorescence analysis. Specifically, the B( $\alpha$ )P groups were compared to the carrier group (DMSO), while groups treated with CNPW alone and in combination with B( $\alpha$ )P were compared to the control. The ANOVA was followed by a Fisher LSD *post-hoc* test to investigate significant differences taking  $p < 0.05$  as significance cut-off. Statistical analyses were carried out using the STATISTICA 7.0 software package.

### **Results and Discussion**

This study evaluated a key issue related to ecotoxicity of carbon-based NMs such as their interactions with environmental pollutants and the toxicological consequences for aquatic organisms.

The interactive effects of CNPs and pollutants in fish have been investigated on early life stages and on adults.<sup>40-43</sup> While these studies clearly highlighted the impacts of NPs on the uptake and relative accumulation of the adsorbed pollutants in the organisms, their effects on toxicity are still controversial since NPs can decrease the contaminants' bioavailability or act as Trojan-horse, raising and/or changing the toxicological behavior of associated pollutants, based also on the physiology of the biological model.<sup>44</sup>

In this context our research aims to understand how the interplay between CNPW and B( $\alpha$ )P influences contaminants accumulation and related toxicity. First we assessed the sorption property of CNPW towards B( $\alpha$ )P and how it reflects on B( $\alpha$ )P uptake by zebrafish embryos. Secondly, we demonstrated that such interaction affects organism stress response pathways and toxic effects of the single pollutants.

### **CNPW characterization and behavior in exposure media**

1  
2  
3 The primary characterization by SEM showed that the bulk CNPW consisted of large aggregates up to 10  
4  $\mu\text{m}$  (Fig 1). The superficial ultrastructure appeared to be made up of graphite-like sheets with variable  
5 dimensions well-packed each other. Furthermore, TEM observation highlighted that the CNPW consisted  
6 also of another component in particulate form with mean diameter of about 20 nm (Fig. 1). Concerning  
7 CNPW behavior in water media, the Z average measured for CNPW suspended in Milli-Q water (1 g/L),  
8 within the *range* 600-1000 nm, indicated a substantial aggregation state. Once in ZFW, a significant  
9 aggregation of CNPW and consequent sedimentation occurred, starting already after 2 h (Fig S1). This  
10 behavior was confirmed by DLS analysis, showing a reduction of size distribution of the CNPW left into the  
11 water column over 24 h (Table 1). Within the exposure experiments, embryos were exposed either to the  
12 finest fraction of CNPW, and also with larger aggregates (Fig. S1). As to surface charge, the  $\zeta$  potential value  
13 of CNPW suspended in Milli-Q water of  $-30.9 \pm 3.05$  mV moved to  $-20.7 \pm 1.15$  mV once CNPW was in  
14 ZFW. The sorption of B( $\alpha$ )P did not affect significantly the hydrodynamic behavior of CNPW (Table 1).

### 15 ***CNPW clean-up and B( $\alpha$ )P sorption***

16 GC-MS/MS analysis showed a great amount of PAHs' impurities on CNPW up to 20 ppm, equal to 0.002%  
17 of total carbon mass. Fifteen PAHs (US EPA) were identified on the CNPW, at the end of the 92 h clean-up,  
18 the PAHs' impurities on CNPW were reduced to 1.4 ppm (Tab S1).

19 After 72 h of contamination with B( $\alpha$ )P, a negligible fraction of the hydrocarbon remained into water,  
20 corresponding to 0.1% of the administered concentration for CNPW + B( $\alpha$ )P 0.01 mg/L, 0.02 % for CNPW  
21 + B( $\alpha$ )P 0.1 mg/L and 0.07 % for CNPW + B( $\alpha$ )P 1 mg/L (Tab. 2). A significant sorption of B( $\alpha$ )P on  
22 CNPW was observed, which covered two orders of magnitude, reflecting the three different concentrations  
23 of B( $\alpha$ )P administered to CNPW. In detail, about 100 % of B( $\alpha$ )P was adsorbed on CNPW at the B( $\alpha$ )P  
24 concentration of 0.1 mg/L. Instead, the percentage of B( $\alpha$ )P recovered on CNPW was 42 % and 33 % at 0.01  
25 mg/L and 1 mg/L, respectively. The different extent of recovery is probably due to the particular  
26 characteristics of the CNPW, which was formed by two different components: one composed of nanometric  
27 graphite-like sheets and another constituted by nanometric particles. Thus, in spite of our attempt to  
28 homogenize the suspensions, they might have adsorbed the B( $\alpha$ )P differently. Despite the significantly  
29 different percentage of recovery of B( $\alpha$ )P sorbed on CNPW, our goal to obtain three CNPW doped with  
30 increasing amount of B( $\alpha$ )P was achieved. Indeed, the amount of B( $\alpha$ )P sorbed on CNPW doped with B( $\alpha$ )P  
31 0.1 mg/L is lower than that adsorbed on CNPW doped with 1 mg/L (111  $\mu\text{g/g}$  vs 335  $\mu\text{g/g}$ ), regardless the %  
32 of recovery. On the basis of these results, we set the B( $\alpha$ )P concentrations corresponding to suspensions  
33 containing 50 mg/L of CNPW (Tab. 2). The CNPW showed high adsorption properties towards organic  
34 compounds, as widely described for carbon-based NPs.<sup>22-25</sup> The observed properties highlight that airborne  
35 NMs can contribute to PAHs transit into the atmosphere, as well as in the water column, representing a  
36 further PAHs source for aquatic environments. Besides, the high sedimentation rate observed within 24 h  
37 highlighted that CNPW could transport PAHs either into the water column and mainly in sediments.

### *CNPW and B( $\alpha$ )P uptake in embryos*

Any mortality or morphological or behavioural alterations have been observed in embryos exposed to contaminants alone and in combination.

Images of whole mount embryos exposed to B( $\alpha$ )P alone showed a dose-dependent increase of B( $\alpha$ )P-fluorescence signal in the trunk muscle (Fig. 2 d, e, f; Fig. 3 p < 0.001). At the highest B( $\alpha$ )P concentration (20  $\mu$ g/L), an intense fluorescence signal was observed also into the yolk sac (fig. 2 f). A different pattern of B( $\alpha$ )P accumulation was shown in embryos treated with CNPW contaminated with B( $\alpha$ )P (Fig. 2 g, h, j), where B( $\alpha$ )P was localized in the trunk muscle but without observe a dose-dependent accumulation (Fig. 3). A higher fluorescence signal was detected at the lower B( $\alpha$ )P concentration (CNPW + B( $\alpha$ )P 0.2  $\mu$ g/L and CNPW + B( $\alpha$ )P 6  $\mu$ g/L) compared to the single exposure (p = 0.001, p = 0.006 respectively), while at the highest one (CNPW + B( $\alpha$ )P 20  $\mu$ g/L) a lower accumulation of B( $\alpha$ )P was measured compared to the B( $\alpha$ )P alone (p < 0.001) and no fluorescence at all was observed in the yolk. The negligible fluorescence observed in all exposure conditions in the eye and cephalic structures is only due to the natural fluorescence of the surface pigment layer present at the head level.

These evidence highlight that, in embryos, the B( $\alpha$ )P distribution results different in dependence to the way of administration, that is alone or adsorbed on CNPW. Indeed, the B( $\alpha$ )P signal followed a dose-dependent increase upon single exposure, while in co-exposure a similar accumulation of the hydrocarbon seemed to occur independently from the administered B( $\alpha$ )P concentrations, confirming that the two contaminants entered together, being associated one to the other. Besides, the potential of CNPW to increase the bioavailability and accumulation of the hydrocarbon is suggested for lower B( $\alpha$ )P concentrations. Though, at the highest concentration, the strong B( $\alpha$ )P signal in the yolk sac, observed after single exposure, could not be detected in embryos exposed to CNPW contaminated with B( $\alpha$ )P. This evidence suggests a different internalization and sorption of B( $\alpha$ )P on CNPW with respect to B( $\alpha$ )P alone dissolved into the exposure medium. When dissolved in water it is likely that B( $\alpha$ )P enters the embryo's body through the epidermis and accumulates into the yolk. When in co-exposure, however, the B( $\alpha$ )P is sequestered on CNPW and forced to follow the conventional uptake route of this physical contaminant, accumulating in other tissues. Indeed, reflection analysis highlighted the presence of CNPW aggregates -as clear white masses- at the gills level (Fig. 4 d, g) and into the digestive tract (Fig. 4 e, f, h, i). The uptake was observed in embryos exposed to CNPW either alone or combined with B( $\alpha$ )P. TEM analysis localized also the nanometric fraction of CNPW in those organs (Fig. 5), confirming these systems as primary sites for the uptake of CNPW, as described for some NPs in other aquatic models.<sup>45-49</sup> The beginning of feeding behavior in zebrafish embryos does not occur at fixed time-point, but only a rough estimate when ingestion of food starts could be established. Certain anatomical conditions have to occur to allow the external feeding: the mouth must have opened sufficiently wide, the digestive tract has to be fully differentiated, the anus must have opened and the swim bladder inflated, to allow the embryos to hunt.<sup>50</sup> At 96 hpf the occurrence of external feeding is unlikely as the digestive tract is not completely developed and the swim bladder is not inflated.<sup>51</sup> Therefore, at this stage,

1  
2  
3 the transit of CNPW in the digestive tract -revealed by microscopy analysis- has been likely due to passive  
4 entrance through the mounth.

5  
6 Our results are in line with other studies describing a carrier role of CNPs for organic pollutants. The  
7 gastrointestinal tract, in particular, proved to be a key tissue for the bioaccessibility of organic pollutants  
8 adsorbed on CNTs, due to the desorption action of pepsin and bile salts.<sup>52</sup> Accordingly, in the medaka  
9 (*Oryzias latipes*), single walled carbon nanotubes (SWCNTs) associated with PhE were first retained in the  
10 digestive tract of fish, and only later, a significant accumulation of PhE was recorded in other organs as liver  
11 and brain due to the release of the hydrocarbon from SWCNTs over time.<sup>28</sup> Nevertheless a study  
12 demonstrated that PhE bound to C<sub>60</sub> resulted bioavailable and bioaccumulated in junior carp (*Cyprinus*  
13 *carpio*) but was not responsible for toxicity -evaluated as ethoxiresorufin-O-deethylase activity- which was,  
14 instead, generated exclusively by the free PhE.<sup>53</sup>

### 15 16 17 18 19 20 21 22 **Effects on genes' transcription and enzymes' activities**

23  
24 In order to assess whether the described interactions could interfere with cellular pathways of individual  
25 contaminants, we evaluated the expression of genes related to the cellular stress response and the activity of  
26 enzymes involved in the antioxidant response machinery.

27  
28 The cytochrome P4501A (CYP1A) is the primary enzyme involved in the first phase of  
29 biotransformation/detoxification of toxic pollutants, such as PAHs.<sup>54</sup> The expression pattern of *cyp1a* has  
30 been extensively investigated in zebrafish embryos, either under physiological condition or exposed to  
31 environmental pollutants.<sup>55,56</sup> Significant transcription of *cyp1a* mRNA has been observed in zebrafish  
32 embryos already at 24 hpf localizing in almost all tissues. The inducibility of *cyp1a* transcription by dioxin-  
33 like pollutants has been also established.

34  
35 An up-regulation of *cyp1a* gene transcription (2.4-, 4.7-, 2.1-folds compared to DMSO) was observed in  
36 embryos exposed to all B( $\alpha$ )P concentrations (Fig. 6), confirming the involvement of the gene in the  
37 metabolism of B( $\alpha$ )P. As we noticed, the gene induction followed a bell shape trend with the highest up-  
38 regulation at B( $\alpha$ )P 6  $\mu$ g/L. Its low induction at the highest tested concentration suggests that the B( $\alpha$ )P  
39 accumulated in the yolk did not undergo metabolic modification. The exposure to all three concentrations of  
40 B( $\alpha$ )P did not modulate *sod1* and *sod2* gene transcription, as well as *hsp70* expression (Fig. 6).

41  
42 A different pattern of gene transcription was observed upon exposure to CNPW alone and combined with  
43 B( $\alpha$ )P. The profile of genes' modulation suggests that the effects at molecular level mainly mirrored those  
44 shown by the physical contaminant rather than by B( $\alpha$ )P, albeit with some differences.

45  
46 CNPW did not affect *cyp1a* expression, which resulted even slightly down-regulated, as well as CNPW +  
47 B( $\alpha$ )P 6  $\mu$ g/L and CNPW + B( $\alpha$ )P 20  $\mu$ g/L (Fig. 6). On the contrary, an increased amount of *cyp1a* mRNA  
48 was observed upon exposure to CNPW + B( $\alpha$ )P 0.2  $\mu$ g/L, albeit with high variability.

49  
50 A down-regulation of *sod1* and *sod2* was observed in embryos exposed to CNPW alone. Whilst no  
51 modulation of *sod1* was shown upon exposure to CNPW combined with B( $\alpha$ )P, a lower level of *sod2* mRNA  
52 was found in embryos exposed to CNPW + B( $\alpha$ )P 0.2  $\mu$ g/L (0.4- folds vs ctrl) and CNPW + B( $\alpha$ )P 6  $\mu$ g/L

(0.4- folds vs ctrl), while *sod2* expression was restored to background level in embryos exposed to CNPW + B( $\alpha$ )P 20  $\mu$ g/L (1.0 folds vs ctrl). Again, a lower *hsp70* mRNA level was noticed in embryos exposed to CNPW, CNPW + B( $\alpha$ )P 6  $\mu$ g/L and CNPW + B( $\alpha$ )P 20  $\mu$ g/L (0.2-, 0.3-, 0.3- folds vs ctrl), while an up-regulation of this gene was found in the CNPW + B( $\alpha$ )P 0.2  $\mu$ g/L group.

Concerning enzymes activities, exposure to B( $\alpha$ )P affected GST activity following a slight bell shape trend (Fig. 7), since the enzyme resulted significantly induced at 6  $\mu$ g/L B( $\alpha$ )P ( $F=144.17$ ;  $p<0.001$ ), while GST was significantly lowered at the highest B( $\alpha$ )P compared to the corresponding control ( $p<0.001$ ). GST is a family of phase II detoxification enzymes that catalyze the conjugation of glutathione to a wide variety of endogenous and exogenous electrophilic compounds, including environmental pollutants and oxidative stress by-products.<sup>57</sup> The increase of GST, which followed a similar trend of *cyp1a* gene, supports an efficient metabolism/excretion of B( $\alpha$ )P out of the cell. A significant increase of GST was observed also in embryos exposed to CNPW alone ( $p<0.001$ ). On the contrary, a significant inhibition of GST activity was measured in all groups exposed to CNPW contaminated with B( $\alpha$ )P ( $p<0.001$ ). Such result underlines that the exposure to combined pollutants could hinder the detoxifying capacity of the embryos. The same evidence was also found in zebrafish hepatocytes after C<sub>60</sub> and B( $\alpha$ )P exposure.<sup>29</sup> Fullerene enhanced B( $\alpha$ )P cellular uptake and decreased GST activity, with consequent induction of cell death.

The oxidative metabolism of pollutants, mediated by CYP1A, could determine the formation of hydroxy radicals and reactive oxygen species (ROS), leading to oxidative stress.<sup>58</sup> To counteract the rise of ROS, the organisms use diverse arrays of enzymes, such as SOD and CAT. A significant activation of CAT activity was found only in embryos exposed to the highest B( $\alpha$ )P concentration ( $F=9.57$ ;  $p=0.03$ ). An increase of SOD activity in zebrafish exposed to increasing B( $\alpha$ )P concentrations, when administered alone, was measured, following a clear bell-shape slope (Fig. 7). The observed increase of SOD and CAT activities confirmed an efficient protective mechanism displayed by the embryos upon exposure to B( $\alpha$ )P, which prevent the onset of oxidative stress condition. On the contrary a significant inhibition of CAT was measured in embryos exposed to CNPW alone ( $p=0.004$ ) and to CNPW + 20  $\mu$ g/L B( $\alpha$ )P ( $p=0.004$ ). CNPW did not affect significantly SOD activity neither alone nor combined with all B( $\alpha$ )P concentrations. Oxidative stress is a widely described toxic effect of NMs, mainly due to ROS overproduction, though the cellular mechanisms are not completely understood, and might vary in relation to different chemico/physical properties of NMs.<sup>59</sup> In aquatic organisms exposed to NMs either induction or depression of SOD and CAT activities have been reported.<sup>60-63</sup> Therefore, the observed misregulation of key genes/proteins related to the antioxidant response, suggest that CNPW alone and combined with B( $\alpha$ )P might induce toxicity through the imbalance of the antioxidant defense mechanism.

Overall, results highlight that, once entered in the organism, the B( $\alpha$ )P adsorbed on CNPW activates cell pathways in a different way with respect to B( $\alpha$ )P alone. In particular the adsorbed B( $\alpha$ )P overcomes the CYP450-mediated detoxification mechanisms and interferes with transcription of genes related to stress response pathways.

### Cyto-genotoxic effects

The different modulation of genes/proteins involved in the cellular protective mechanisms, elicited by CNPW contaminated with B( $\alpha$ )P with respect to the two pollutants alone, might have reduced the detoxifying capacity of the organism, reflecting in unexpected adverse consequences, such as for instance an increase of cyto-genotoxicity.

We did not find any significant cytotoxic effect at all B( $\alpha$ )P and CNPW experiments with respect to controls (DMSO for B( $\alpha$ )P; ZFW for CNPW) (Fig. 8). Besides, MN analysis showed a very low frequency of micronucleated cells (< 3 %) and no effect on MN frequency was revealed upon all exposure conditions (F = 1.69; p = 0.12; data not shown).

The exposure to B( $\alpha$ )P determined a significant increase (F=3.46; p<0.01) of DNA fragmentation only at the intermediate concentration (6  $\mu$ g/L; Fig. 8). Any fixed genetic damage was observed in embryos exposed to all B( $\alpha$ )P concentrations (Fig. 8). The low genotoxicity observed for B( $\alpha$ )P, followed a trend similar to *cyp1a* gene modulation. The genotoxic properties of high-molecular-weight PAHs such as B( $\alpha$ )P are commonly associated with their biotransformation/detoxification.<sup>64</sup> In particular CYP1A is able to convert PAHs to reactive intermediates which have the ability to interact with DNA, causing adducts.<sup>65</sup> In line with this evidence, our results suggested that a relationship could be established between CYP1A detoxifying activity and occurrence of primary DNA damage.

Anyhow the observed induction of CYP1A was not enough to produce a significant bioactivation of chemical. Besides, the short time of exposure (72 h) may have contributed to the absence of genotoxic effects, particularly the occurrence of micronucleated cells.

Any genetic injury was detected in embryos exposed to CNPW alone (Fig. 8). To date, the genotoxicity of carbon-based NPs have been investigated mostly on *in vitro* mammalian models,<sup>32</sup> but barely assessed *in vivo* on aquatic organisms, and the mechanisms underlying genotoxicity are far to be understood. Any fixed genotoxic effect -measured as MN occurrence- has been observed in the amphibian *X. leavis* erythrocytes, upon exposure to CNTs (10 mg/L) for 12 days.<sup>66</sup> On the contrary, the occurrence of apoptotic and necrotic cells has been detected in zebrafish embryos exposed to C<sub>60</sub> (0.05-0.1-0.2 mg/L) for 12 h, affecting also the embryo development.<sup>67,68</sup> The genotoxicity of CB (Printex 90) has been investigated in haemocytes of the bivalve *M. galloprovincialis*,<sup>8</sup> in which the nano-CB increased the release of hydrolytic enzymes and mitochondrial damage, enhancing the onset of pre-apoptotic events. In line with this evidence, the down-regulation of genes related to the cellular stress response (*sod1*, *sod2*, *hsp70*) and the reduction of the antioxidant enzyme CAT, highlight the genotoxic potential of CNPW. Nevertheless, the experimental conditions might have hindered the onset of genetic damage as observed for B( $\alpha$ )P. Besides, the increase of GST activity could allow counteracting the occurrence of cyto-genotoxic effects upon single exposure.

Although the exposure to individual contaminants did not induce cyto-genotoxic damage to embryos, when molecules were administered in co-exposure, a significant increase in toxicity was observed. The embryos exposed to CNPW combined with B( $\alpha$ )P showed a dose-dependent reduction of cell viability (F=6.86; p<0.001), up to 25% at the highest B( $\alpha$ )P dose. Despite the observed cytotoxicity, the cell viability remained

1  
2  
3 higher than 70% in all exposures, which is the threshold required to perform further genotoxicity tests.<sup>69</sup>  
4 Embryos exposed to CNPW combined with all the three doses of B( $\alpha$ )P showed a significantly higher  
5 percentage of DNA in comet tail than that found in individuals treated with CNPW alone (about 7%  $p <$   
6 0.01). In addition, the onset of fixed genetic damage with respect to the controls was observed. Embryos  
7 treated with CNPW combined with B( $\alpha$ )P showed an increase in the % of apoptotic cells, which resulted  
8 significantly higher compared to control and to CNPW alone in CNPW + B( $\alpha$ )P 6  $\mu\text{g/L}$  group ( $F = 22.47$ ;  $p$   
9  $< 0.001$ ). Similarly, a higher percentage of necrotic cells was measured in embryos exposed to CNPW +  
10 B( $\alpha$ )P 20  $\mu\text{g/L}$  with respect to controls and CNPW alone ( $F = 5.07$ ;  $p < 0.001$ ).

11  
12 These results confirm that the alteration of genes/proteins, related to the cellular stress response observed  
13 upon exposure to combined pollutants, reflect in higher cyto/genotoxicity for embryos.

14  
15 The occurrence of cyto-genotoxic effects in embryos exposed to CNPW contaminated with B( $\alpha$ )P might be  
16 due to ROS production that overcomes the scavenging capacity of the antioxidative system, as suggested by  
17 the down-regulation of *sod* genes and the significant inhibition of GST. Moreover, the down-regulation of  
18 *hsp70* transcription might explain the occurrence of apoptotic events in co-exposed embryos, as this  
19 molecular chaperone is actively involved in cellular response related to stress resistance, providing cyto-  
20 protective function against apoptosis.<sup>70</sup>

21  
22 The cellular responses obtained in co-exposure conditions suggested that the B( $\alpha$ )P adsorbed contributes to  
23 increase the toxicity of CNPW, producing a greater toxic effect compared to the damage caused by the  
24 individual contaminants, as already described for carbon-based NPs combined with PAHs. For instance, the  
25 co-exposure of C<sub>60</sub> (0.10 to 1 mg/L) and fluoranthene (32-100 mg / L) for 72 hours, increased the DNA  
26 fragmentation compared to individual contaminants in *M. galloprovincialis*.<sup>9</sup> The increase of the  
27 genotoxicity might also be related to higher bioavailability and retention of B( $\alpha$ )P, which is translocated  
28 inside the embryos by CNPW as shown by confocal images.

## 39 Conclusions

40  
41 Overall, our results open a new light in the possible relationship of NMs and pollutants in the aquatic  
42 environment. In particular, our findings highlighted the interaction with contaminants as key feature of NMs  
43 ecotoxicity. In fact the adsorption properties of CNPW for B( $\alpha$ )P suggested that NM act as vehicle of toxic  
44 pollutants in the aquatic ecosystems. CNPW is also able to interfere with cell stress/detoxification  
45 mechanisms, thereby affecting the organism susceptibility to chemical pollutants. Therefore, single or  
46 combination of CNPW and B( $\alpha$ )P induce different cellular metabolic responses respect to single exposure,  
47 enhancing the occurrence of cyto-genotoxic effects, affecting different intracellular pathways. Further studies  
48 focusing on specific molecular pathways are prompted, to get an in-depth knowledge of the relationship  
49 between CNPW and one of the most toxic environmental pollutants. The sorption properties of CNPW  
50 towards organic pollutants, pointed out in the present study, arouse concern also in terms of the possible  
51 negative effects on human health. Carbon-based nanopowder represents, in fact, one of the main components  
52 of PM 2.5 and therefore could contribute to enhance the uptake of airborne noxious contaminants in human,  
53  
54  
55  
56  
57  
58  
59  
60

with unexpected toxicological consequences.

### Acknowledgements

This study was financially supported by the “Cariplo Foundation” grant number 2013-0817.

### Author contribution

C.D.T. and M.P. designed and performed experiments, analysed data and wrote the paper. A.B. is the supervisor and leader of the study. L.D.G. supervised qRT-PCR analysis. A.G. designed and performed qRT-PCR analysis and edited the paper. M.A. designed and performed confocal microscopy analysis. N.S. supervised microscopy analysis. D.M. designed and performed DLS analysis and gave conceptual advice for characterization. L.M. performed confocal microscopy analysis. S.M. and L.P. gave technical support and conceptual advice. C.L.P. gave conceptual advice. A.B., L.D.G., N.S. and C.L.P. jointly conceived the study and edited the paper.

### References

1. G. Brumfield, A little knowledge...., *Nature*, 2003, **424**, 246-248.
2. P. A. Holden, R. M. Nisbet, H. S. Lenihan, R. J. Miller, G. N. Cherr, J. P. Schimel and J. L. Gardea-Torresdey, Ecological Nanotoxicology: Nanomaterial hazard considerations at the subcellular, population, community, and ecosystems levels. *Acc. Chem. Res.*, 2013, **46**, 813-822.
3. B. Nowack and T. D. Bucheli, Occurrence, behavior, and effects of nanoparticles in the environment, *Environ. Pollut.*, 2007, **150**, 5-22.
4. I K. L. Gardner and A. A. Keller, Emerging patterns for engineered nanomaterials in the environment: a review of fate and toxicity studies, *J. Nanopart. Res.*, 2014, **16**, 2503-2531.
5. M. A. Maurer-Jones, I. L. Gunsolus, C. J. Murphy and C. L. Haynes, Toxicity of engineered nanoparticles in the environment, *Anal. Chem.*, 2013, **85**, 3036-3049.
6. I. Corsi, G. N. Cherr, H. S. Lenihan, J. Labille, M. Hasselov, L. Canesi, F. Dondero, G. Frenzilli, D. H. Hristozov, V. Puentes, C. Della Torre, Common strategies and technologies for the ecosafety assessment and design of nanomaterials entering the marine environment. *ACS Nano*, 2014, **8**, 9694-9709.
7. S. Pérez, M. Farré and D. Barceló, Analysis: behaviour and ecotoxicity of carbon-based nanomaterials in the aquatic environment, *Trends Anal. Chem.*, 2009, **28**, 820-832.
8. L. Canesi, C. Ciacci, M. Betti, R. Fabbri, B. Canonico, A. Fantinati, A. Marcomini, and G. Pojana. Immunotoxicity of carbon black nanoparticles to blue mussel hemocytes, *Environ. Int.*, 2008, **34**, 1114-1119.
9. A. D. Arndt, J. Chen, M. Moua and R. D. Klaper, Multigeneration impacts on *Daphnia magna* of carbon nanomaterials with differing core structures and functionalization, *Environ. Toxicol. Chem.*, 2013, **33**, 541-547.



- 1  
2  
3  
4  
5  
6  
7  
8  
9  
10  
11  
12  
13  
14  
15  
16  
17  
18  
19  
20  
21  
22  
23  
24  
25  
26  
27  
28  
29  
30  
31  
32  
33  
34  
35  
36  
37  
38  
39  
40  
41  
42  
43  
44  
45  
46  
47  
48  
49  
50  
51  
52  
53  
54  
55  
56  
57  
58  
59  
60
10. E. K. Sohn, Y. S. Chung, S. A. Johari, T. G. Kim, J. K. Kim, H. J. Lee, Y. H. Lee, S. W. Kang and I. J. Yu, Acute toxicity comparison of single-walled carbon nanotubes in various freshwater organisms, *BioMed Res. Int.*, 2015, DOI: 10.1155/2015/323090.
  11. K. T. Kim, M. H. Jang, J. Y. Kim, B. S. Xing, R. L. Tanguay, B. G. Lee and S. D. Kim, Embryonic toxicity changes of organic nanomaterials in the presence of natural organic matter, *Sci. Total. Environ.*, 2012, **426**, 423-429.
  12. T. Mesaric, C. Gambardella, T. Milivojevic, M. Faimali, D. Drobne, C. Falugi, D. Makovec, A. Jemec and K. Sepcic, High surface adsorption properties of carbon-based nanomaterials are responsible for mortality, swimming inhibition, and biochemical responses in *Artemia salina* larvae, *Aquat. Toxicol.*, 2015, **163**, 121-129.
  13. J. Li, G-G. Ying, K. C. Jones and F. L. Martin, Real-world carbon nanoparticle exposures induce brain and gonadal alterations in zebrafish (*Danio rerio*) as determined by biospectroscopy techniques, *Analyst*, 2015, **140**, 2687-2695.
  14. S. N. Al-Subiai, V. M. Arlt, P. E. Frickers, J. W. Readman, B. Stolpe, J. R. Lead, A. J. Moody and A. N. Jha Merging nano-genotoxicology with eco-genotoxicology: an integrated approach to determine interactive genotoxic and sub-lethal toxic effects of C(60) fullerenes and fluoranthene in marine mussels, *Mytilus sp.*, *Mutat. Res.*, 2012, **745**, 92-103.
  15. L. Canesi, C. Ciacci and T. Balbi, Interactive effects of nanoparticles with other contaminants in aquatic organisms: Friend or foe?, *Mar. Environ. Res.* 2015, **111**, 128-134.
  16. C. Della Torre, T. Balbi, G. Grassi, G. Frenzilli, N. Bernardeschi, A. Smerilli, P. Guidi, L. Canesi, M. Nigro, F. Monaci, V. Scarcelli, L. Rocco, S. Focardi, M. Monopoli and I. Corsi, Titanium dioxide nanoparticles modulate the toxicological response to cadmium in the gills of *Mytilus galloprovincialis*, *J. Haz. Mat.*, 2015, **297**, 92-100.
  17. C. Della Torre, F. Buonocore, G. Frenzilli, S. Corsolini, A. Brunelli, P. Guidi, A. Kocan, M. Mariottini, F. Mottola, M. Nigro, K. Pozo, E. Randelli, M. L. Vannuccini, S. Picchietti, M. Santonastaso, V. Scarcelli, S. Focardi, A. Marcomini, L. Rocco, G. Scapigliati and I. Corsi, Influence of Titanium Dioxide Nanoparticles on 2,3,7,8-Tetrachlorodibenzo-*p*-dioxin Bioconcentration and Toxicity in the marine fish European sea bass (*Dicentrarchus labrax*), *Environ. Pollut.* 2015, **196**, 185-193.
  18. B. Glomstad, D. Altin, L. Sorensen, J. Liu, B. M. Jenssen and A. M. Booth, Carbon nanotube properties influence adsorption of phenanthrene and subsequent bioavailability and toxicity to *Pseudokirchneriella subcapitata*, *Environ. Sci. Technol.* 2016, **50**, 2660-2668.
  19. Baun, S. N. Sorensen, R. F. Rasmussen, N. B. Hartmann and C. B. Koch, Toxicity and bioaccumulation of xenobiotic organic compounds in the presence of aqueous suspensions of aggregates of nano-C-60, *Aquat. Toxicol.*, 2008, **86**, 379-387.
  20. F. Schwab, T. D. Bucheli, L. Camenzuli, A. Magrez, K. Knauer, L. Sigg and B. Nowack, Diuron sorbed to carbon nanotubes exhibits enhanced toxicity to *Chlorella vulgaris*, *Environ. Sci. Technol.*, 2013, **47**, 7012-7019. □

21. X.Y., Yang, R. E. Edelman and J. T. Oris, Suspended C60 nanoparticles protect against short-term UV and fluoranthene photo-induced toxicity, but cause long-term cellular damage in *Daphnia magna*, *Aquat. Toxicol.*, 2010, **100**, 202-210.
22. Y. Watson and P. A. Walberg, Carbon black and soot: Two different substances, *Am. Indus. Hygen. Ass. J.*, 2001, **62**, 218-228.
23. K. Yang, X. Wang, L. Zhu and B. Xing, Competitive sorption of pyrene, phenanthrene and naphthalene on multiwalled carbon nanotubes. *Environ. Sci. Technol.*, 2006, **40**, 5804-5810.
24. X. L. Hu, J. F. Liu, P. Mayer and G. B. Jiang, Impacts of some environmentally relevant parameters on the sorption of polycyclic aromatic hydrocarbons to aqueous suspensions of fullerene, *Environ. Toxicol. Chem.*, 2008, **27**, 1868-74.
25. X. Hu, J. Li, Q. Chen, Z. Lin and D. Yin, Combined effects of aqueous suspensions of fullerene and humic acid on the availability of polycyclic aromatic hydrocarbons: evaluated with negligible depletion solid-phase microextraction, *Sci. Tot. Environ.*, 2014, **493**, 12-21.
26. E. J. Petersen, R. A. Pinto, P. F. Landrum and W. J., Jr. Weber, Influence of Carbon Nanotubes on Pyrene Bioaccumulation from Contaminated Soils by Earthworms, *Environ. Sci. Technol.* 2009, **43**, 4181-4187.
27. A. L. Rodd, M. A. Creighton, C. A. Vaslet, J. R. Rangel-Mendez, R. H. Hurt and A. B. Kane, Effects of surface-engineered nanoparticle-based dispersants for marine oil spills on the model organism *Artemia franciscana*, *Environ. Sci. Technol.*, 2014, **48**, 6419-6427.
28. Y. Su, X. M. Yan, Y. B. Pu, F. Xiao, D. S. Wang and M. Yang, Risks of Single-Walled Carbon Nanotubes Acting as Contaminants- Carriers: Potential Release of Phenanthrene in Japanese Medaka (*Oryzias latipes*), *Environ. Sci. Technol.*, 2013, **47**, 4704-4710
29. J. L. Ferreira, M. N. Lonne, T. A. França, N. R. Maximilla, T. H. Lugokenski, P. G. Costa, G. Fillmann, F. A. Soares, F. R. de la Torre and J. M. Monserrat, Co-exposure of the organic nanomaterial fullerene C60 with benzo[a]pyrene in *Danio rerio* (zebrafish) hepatocytes: evidence of toxicological interactions, *Aquat. Toxicol.* 2014, **147**, 76-83.
30. A. Nel, T. Xia, L. Madler, and L. Ning, Toxic potential of materials at the nanolevel. *Science* 2006, **311**, 622-627.
31. Z. Magdolenova, A. Collins, A. Kumar, A. Dhawan, V. Stone and M. Dusinska, Mechanisms of genotoxicity. A review of in vitro and in vivo studies with engineered nanoparticles, *Nanotoxicology*, 2014, 8:3, 233-278.
32. N. D. Lawson and B. M. Weinstein, *In vivo* imaging of embryonic vascular development using transgenic zebrafish, *Dev. Biol.* 2002, **248**, 307-318.
33. A. Bui, Z. Perveen, K. Kleinow and Penn A, Zebrafish embryos sequester and retain petrochemical combustion products: developmental and transcriptome consequences. *Aquat. Toxicol.*, 2012, **108**, 23-32.

- 1  
2  
3  
4  
5  
6  
7  
8  
9  
10  
11  
12  
13  
14  
15  
16  
17  
18  
19  
20  
21  
22  
23  
24  
25  
26  
27  
28  
29  
30  
31  
32  
33  
34  
35  
36  
37  
38  
39  
40  
41  
42  
43  
44  
45  
46  
47  
48  
49  
50  
51  
52  
53  
54  
55  
56  
57  
58  
59  
60
34. S. R. Subashchandrabose, K. Krishnan, E. Gratton, M. Megharaj, Naidu, R., Potential of fluorescence imaging techniques to monitor mutagenic PAH uptake by microalga. *Environ. Sci. Technol.*, 2014, **48**, 9152-9160.
35. M. Bradford, A rapid and sensitive method for the quantitation of microgram quantities of protein utilizing the principle of protein-dye binding, *Anal. Biochem.* 1976, **72**, 248-254.
36. M. Parolini, A. Binelli, D. Cogni and A. Provini, Multi-biomarker approach for the evaluation of the cyto-genotoxicity of paracetamol on zebra mussel (*Dreissena polymorpha*), *Chemosphere*, 2010, **79**, 489–498.□
37. T. Kosmehl, A. V. Hallare, T. Braunbeck and H. Hollert, DNA damage induced by genotoxicants in zebrafish (*Danio rerio*) embryos after contact exposure to freeze-dried sediment and sediment extracts from Laguna Lake (The Philippines)□as measured by the comet assay, *Mutat. Res.* 2008, **650**, 1-14.
38. N. P. Singh, Microgels for estimation of DNA strand breaks, DNA protein crosslinks and apoptosis, *Mutat. Res.*, 2010, **455**, 111–127.
39. M. Pavlica, G.I.V. Klobucar, N. Vetma, R. Erben and D. Papeš, Detection of micronuclei in haemocytes of zebra mussel and ramshorn snail exposed to pentachlorophenol, *Mutat. Res.*, 2010, **465**, 145–150.
40. J. W. Park, T. B. Henry, F. M. Menn, R. N. Compton and G. Sayler, No bioavailability of 17  $\alpha$ -ethinylestradiol when associated with nc(60) aggregates during dietary exposure in adult male zebrafish (*Danio rerio*), *Chemosphere*, 2010, **81**, 1227-1232.
41. J. W. Park, T. B. Henry, S. Ard, F. M. Menn, R. N. Compton and G. S. Sayler, The association between nC(60) and 17  $\alpha$ - ethinylestradiol (EE2) decreases EE2 bioavailability in zebrafish and alters nanoaggregate characteristics, *Nanotoxicology*, 2011, **5**, 406–416.
42. J. Campos-Garcia, D. S. T. Martinez, O. L. Alves, A. F. G., Leonardo and E. Barbieri, Ecotoxicological effects of carbofuran and oxidised multiwalled carbon nanotubes on the freshwater fish *Nile tilapia*: Nanotubes enhance pesticide ecotoxicity, *Ecotoxicol. Environ. Saf.*, 2015, **111**, 131-137.
43. J. R. Falconer, C.F. Jones, S. Lu and D. W. Grainger, Carbon nanomaterials rescue phenanthrene toxicity in zebrafish embryo cultures, *Environ. Sci. Nano*, 2015, **2**, 645-652.
44. J. Sanchis, M. Olmos, P. Vincent, M. Farrè, and D. Barcelo, New Insights on the Influence of Organic Co-Contaminants on the Aquatic Toxicology of Carbon Nanomaterials, *Environ. Sci. Technol.*, 2016, **50**, 961-969.
45. S. Böhme, H-J. Stärk, D. Kühnel and T. Reemtsma, Exploring LA-ICP-MS as a quantitative imaging technique□ to study nanoparticle uptake in *Daphnia magna* and zebrafish (*Danio rerio*) embryos, *Anal. Bioanal. Chem.*, 2015, **407**, 5477–5485.
46. C. Della Torre, E. Bergami, A. Salvati, C. Faleri, P. Cirino, A. K. Dawson and I. Corsi , Uptake, disposition and toxicity of Polystyrene Nanoparticles in sea urchin embryos *Paracentrotus lividus*, *Environ. Sci. Technol.*, 2014, **48**, 12302-12311.
47. E. Bergami ,E. Bocci, M. L. Vannuccini, M. Monopoli, A. Salvati, K. A. Dawson and I. Corsi, Nano-sized polystyrene affects feeding, behavior and physiology of brine shrimp *Artemia franciscana* larvae.

- 1  
2  
3  
4  
5  
6  
7  
8  
9  
10  
11  
12  
13  
14  
15  
16  
17  
18  
19  
20  
21  
22  
23  
24  
25  
26  
27  
28  
29  
30  
31  
32  
33  
34  
35  
36  
37  
38  
39  
40  
41  
42  
43  
44  
45  
46  
47  
48  
49  
50  
51  
52  
53  
54  
55  
56  
57  
58  
59  
60
- Ecotoxicol. Environ. Saf.*, 2016, **123**, 18-25.
48. R. Bacchetta, P. Tremolada, C. Di Benedetto, N. Santo, U. Fascio, G. Chirico, A. Colombo, M. Camatini and P. Mantecca, Does carbon nanopowder threaten amphibian development?, *Carbon*, 2012, **50**, 4607-4618.
49. J. Moger, B.D. Johnston and C. Tyler, Imaging metal oxide nanoparticles in biological structures with CARS microscopy, *Opt. Express.*, 2008, **16**, 3408-3419.
50. S. E. Belanger, E. K. Balon and J. M. Rawlings, Saltatory ontogeny of fishes and sensitive early life stages for ecotoxicological tests. *Aquat. Toxicol.*, 2010, **97**, 88-95.
51. C. B. Kimmel, W. W. Ballard, S. R. Kimmel, B. Ullman and T. F. Schilling, Stages of embryonic development of the zebrafish. *Dev. Dynam.*, 1995, **203**, 253–310.
52. Z. Wang, J. Zhao, L. Song, H. Mashayekhi, B. Chefetz and B. Xing, Adsorption and Desorption of Phenanthrene on Carbon Nanotubes in Simulated Gastrointestinal Fluids, *Environ. Sci. Technol.*, 2011, **45**, 6018-6024.
53. X. Hu, J. Li, Q. Chen and D. Yin, Fullerene-associated phenanthrene contributes to bioaccumulation but is not toxic to fish, *Environ. Toxicol. Chem.*, 2015, **34**, 1023-1030.
54. C. Della Torre, A. Tornambè, S. Cappello, M. Mariottini, G. Perra, S. Giuliani, E. Amato, C. Falugi, A. Crisari, M. Yakimov and E. Magaletti, Modulation of CYP1A and genotoxic effects in European seabass (*Dicentrarchus labrax*) exposed to weathered oil: a mesocosm study, *Mar. Environ. Res.*, 2012, **76**, 48-55.
55. E. A. Andreasen, J. M. Spitsbergen, R. L. Tanguay, J. J. Stegeman, W. Heideman and R. E. Peterson, Tissue-specific expression of AHR2, ARNT2, and CYP1A in zebrafish embryos and larvae: effects of developmental stage and 2,3,7,8-tetrachlorodibenzo-p- dioxin exposure. *Toxicol Sci.*, 2002, **68**, 403–419.
56. H. Liu, F-N Nie, H-Y Lin, X-H Ju, J-J Chen and R. Gooneratne, Developmental Toxicity, EROD, and CYP1A mRNA Expression in Zebrafish Embryos Exposed to Dioxin-Like PCB126. *Environ. Toxicol.*, 2014, **31**, 201-210.
57. R. van der Oost, J. Beyer and N.P.E. Vermeulen, Fish bioaccumulation and biomarkers in environmental risk assessment: a review, *Environ. Toxicol. Pharmacol.*, 2003, **13**, 57–149.
58. J. J. Schlezinger and J.J., Stegeman, Induction of cytochrome P450 1A in the American eel by model halogenated and non-halogenated aryl hydrocarbon receptor agonists, *Aquat. Toxicol.*, 2000, **50**, 375–386.
59. A. Manke, L. Wang and Y. Rojanasakul, Mechanisms of nanoparticle-induced oxidative stress and toxicity, *Biomed. Res. Int.* 2013 (942916), 15.
60. L. Hao, Z. Wang, and B. Xing, Effect of sub-acute exposure to TiO<sub>2</sub> nanoparticles on oxidative stress and histopathological changes in Juvenile Carp (*Cyprinus carpio*). *J. Environ. Sci.*, 2009, **21**, 1459-1466.
- T. Gomes, J. P. Pinheiro, I. Cancio, C. G. Pereira, C. Cardoso and M. J. Bebianno, Effects of copper nanoparticles exposure in the Mussel *Mytilus galloprovincialis*, *Environ. Sci. Technol.*, 2011, **45**, 9356–

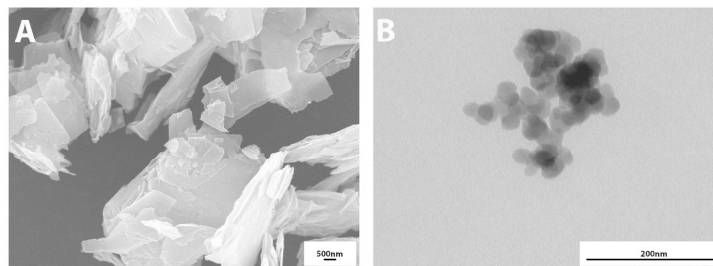
9362. □
62. Z. Clemente, V. L. S. S. Castro, M. A. M. Moura, C. M. Jonsson and L. F. Fraceto, Toxicity assessment of TiO<sub>2</sub> nanoparticles in zebrafish embryos under different exposure conditions, *Aquat. Toxicol.*, 2014, **147**, 129-139.
63. M. Chen, J. Yin, Y. Liang, S. Yuan, F. Wang, M. Song and H. Wang, Oxidative stress and immunotoxicity induced by graphene oxide in zebrafish, *Aquat. Toxicol.* 2016, **174**, 54-60.
64. J. J. Stegeman and J.J. Lech, Cytochrome-P-450 monooxygenase systems in aquatic species—carcinogen metabolism and biomarkers for carcinogen and pollutant exposure, *Environ. Health Perspect.*, 1991, **90**, 101–109.
65. M. Oliveira, M. Pacheco and M. A. Santos, Cytochrome P4501A, genotoxic and stress responses in golden grey mullet (*Liza aurata*) following short-term exposure □to phenanthrene, *Chemosphere*, 2007, **66**, 1284-1291.
66. F. Mouchet, P. Landois, V. Datsyuk, P. Puech, E. Pinelli, E. Flahaut, and L. Gauthier, International amphibian micronucleus standardized procedure (ISO 21427-1) for in vivo evaluation of double-walled carbon nanotubes toxicity and genotoxicity in water, *Environ. Toxicol.*, 2011, **26**, 136–145.
67. C. Y. Usenko, S. L. Harper and R. L., Tanguay, In vivo evaluation of carbon fullerene toxicity using embryonic zebrafish, *Carbon*, 2007, **45**, 1891–8. □
68. C. Y. Usenko, S. L. Harper and R. L., Fullerene C<sub>60</sub> exposure elicits an oxidative stress response in embryonic zebrafish, *Toxicol Appl Pharmacol.*, 2008, **229**, 44–55.
69. D. J. Kirkland, D. Hayashi, M. Jacobson-Kram, P. Kasper, J. T. MacGregor, L. Müller and Y. Uno, Summary of major conclusions from the 4th IWGT, San Francisco, 9–10 September, *Mutat. Res.*, 2007, **627**, 5–9.
70. A-L. Rerole, G. Jegou and C. Garrido, Hsp70: Anti-apoptotic and Tumorigenic Protein, *Mol. Chap.*, 2011, **787**, 205-230.

**Table 1.** DLS measurements performed on CNPW alone in MILLIQ and CNPW contaminated with growing amounts of B( $\alpha$ )P in zebrafish water:  $\zeta$ -potential (mV) and mean size distribution (nm).

Sample	$\zeta$ -potential mV	Z average nm (size range)		
		2 h	4 h	24 h
CNPW 50 mg/L	-20.7 $\pm$ 1.15	356 (271 – 482)	167 (133-224)	73.1 (23-130)
CNPW + B( $\alpha$ )P 0.2 $\mu$ g/L	-20.5 $\pm$ 3.58	408 (245 – 589)	186 (123 –275)	172 (26-447)
CNPW + B( $\alpha$ )P 6 $\mu$ g/L	-20.0 $\pm$ 1.59	330 (242 – 405)	231 (78-530)	202 (149-263)
CNPW + B( $\alpha$ )P 20 $\mu$ g/L	-20.1 $\pm$ 3.12	419 (171 – 445)	267 (163 – 495)	282 (97-396)

**Table 2.** Results of GC/MS analyses of supernatant and CNPW fraction after contamination of cleaned CNPW with increasing amounts of B( $\alpha$ )P.

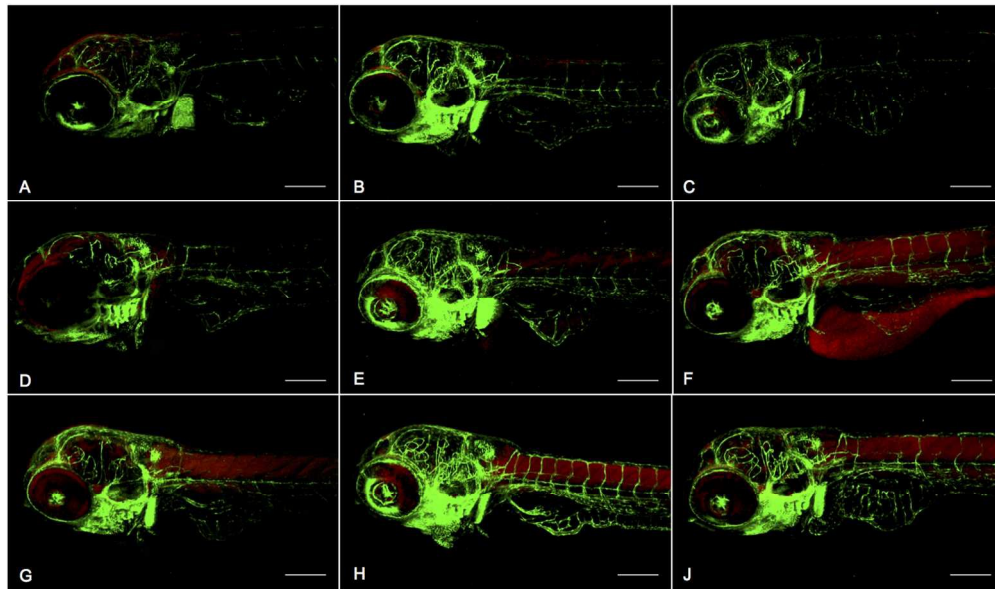
Sample	$\mu$ g B( $\alpha$ )P /L water	$\mu$ g B( $\alpha$ )P /g CNPW	$\mu$ g B( $\alpha$ )P /50 mg CNPW
CNPW + B( $\alpha$ )P 0.01 mg/L	0.02	4.22	0.21
CNPW + B( $\alpha$ )P 0.1 mg/L	0.02	111.34	5.57
CNPW + B( $\alpha$ )P 1 mg/L	0.71	344.62	17.23



Characterization of CNPW at SEM and TEM

209x297mm (300 x 300 DPI)

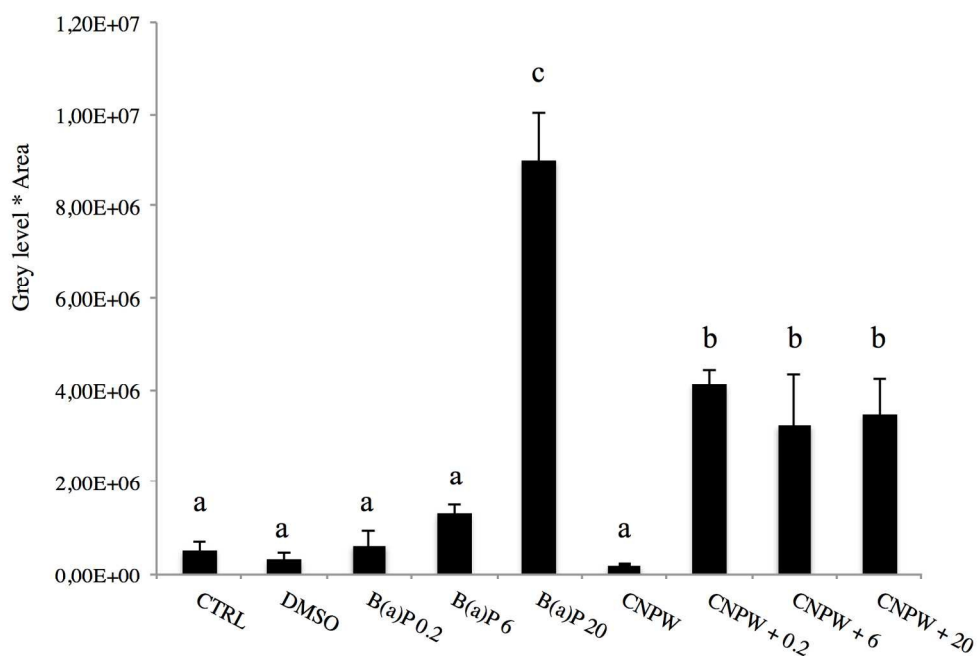
1  
2  
3  
4  
5  
6  
7  
8  
9  
10  
11  
12  
13  
14  
15  
16  
17  
18  
19  
20  
21  
22  
23  
24  
25  
26  
27  
28  
29  
30  
31  
32  
33  
34  
35  
36  
37  
38  
39  
40  
41  
42  
43  
44  
45  
46  
47  
48  
49  
50  
51  
52  
53  
54  
55  
56  
57  
58  
59  
60



Confocal microscopy showing accumulation of B(a)P (red) in zebrafish fli-embryos (96 hpf) showing the vascular system in green. (a) CTRL (b) DMSO (c) CNPW (50 mg/L) (d) B(a)P 0.2 µg/L (e) B(a)P 6 µg/L (f) B(a)P 20 µg/L (g) CNPW + B(a)P 0.2 µg/L (h) CNPW + B(a)P 6 µg/L (i) CNPW + B(a)P 20 µg/L. Scale bar: 200 µm.

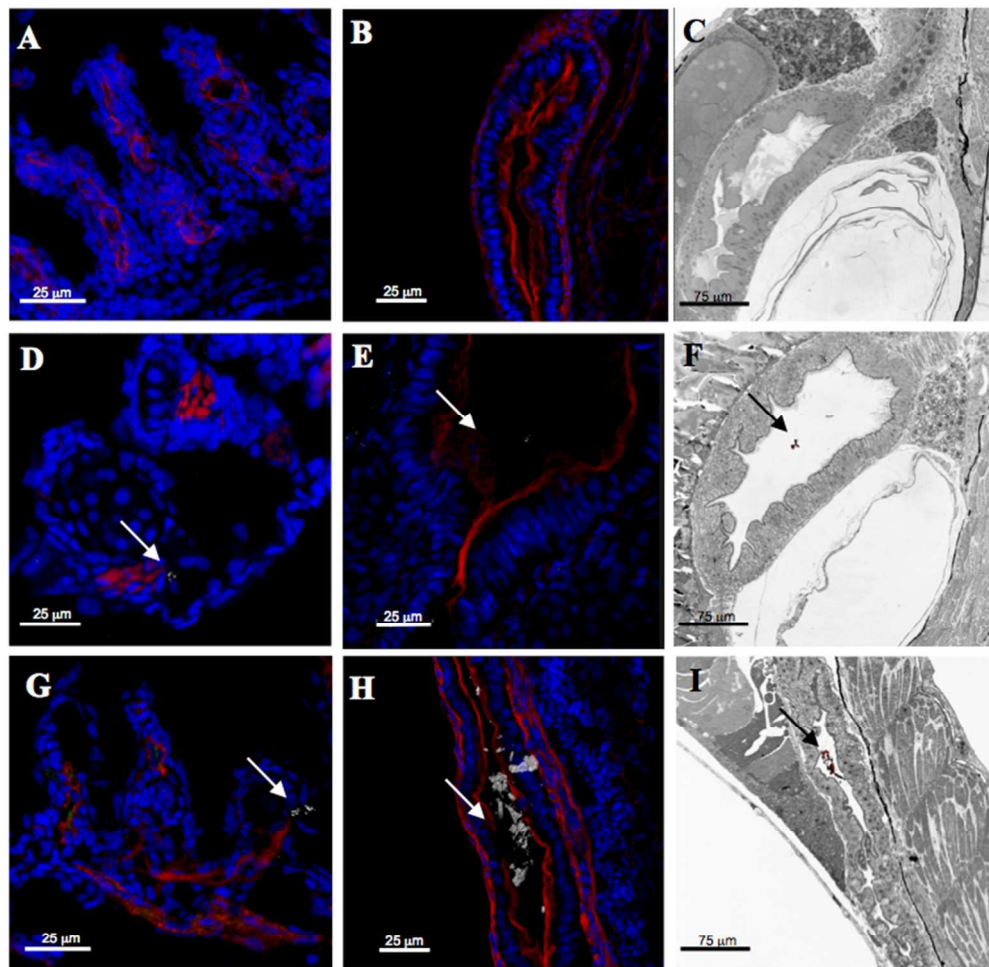
257x151mm (150 x 150 DPI)





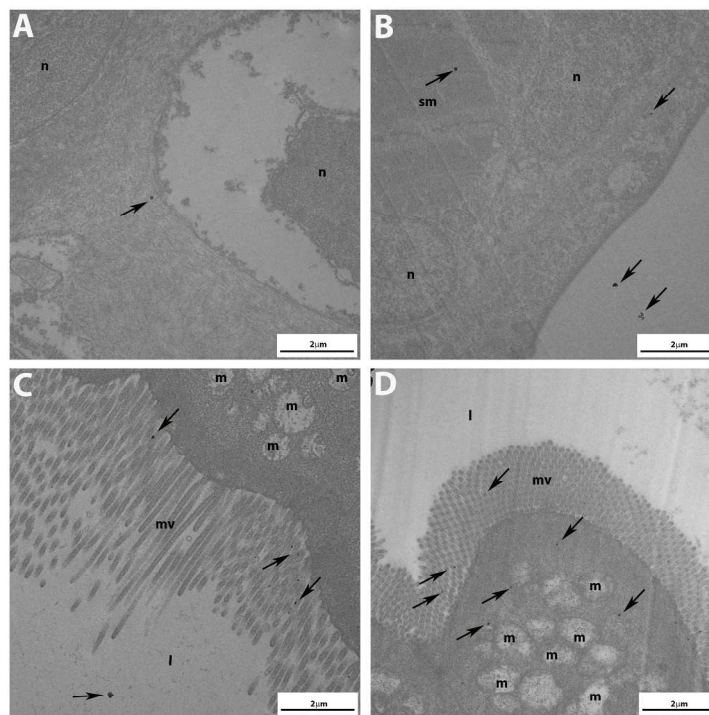
Quantitative fluorescence analysis of B(a)P accumulated in zebrafish embryos (96 hpf) exposed to CNPW (50 mg/L) and B(a)P (0.2, 6, 20  $\mu\text{g/L}$ ) alone and in combination measured as mean ( $\pm$  SEM) of Grey Level x Area ( $\text{pixel}^2$ ). Different letters indicate significantly different values (one-way ANOVA, Fischer's LSD post hoc test;  $p < 0.05$ ).

163x111mm (300 x 300 DPI)



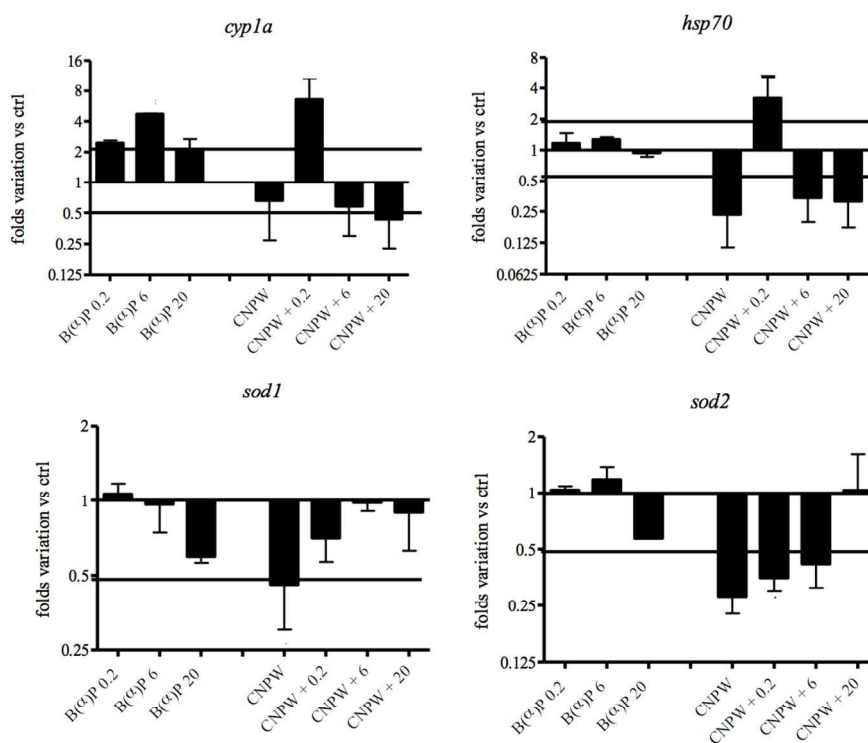
Images of cryostat sections showing the uptake of CNPW -indicated by arrows- in gills (A,D,G) and digestive apparatus (B,C,E,F,H,I) of zebrafish embryos. Controls (A-C), CNPW (D-F) and CNPW + B(a)P 20  $\mu\text{g/L}$  (G-H). DNA in blue (DAPI) (nuclei), musculature in red (phalloidin-TRITC).

129x134mm (150 x 150 DPI)



TEM images showing CNPW indicated by arrows, in gills (A,B) and gastrointestinal tract (C,D) of embryos exposed to CNPW (50 mg/L) (B,D) and CNPW + B(α)P 20 μg/L (A,C). N = nucleus, sm = somatic muscle, m = mitochondrion, l = lumen, mv = microvilli.

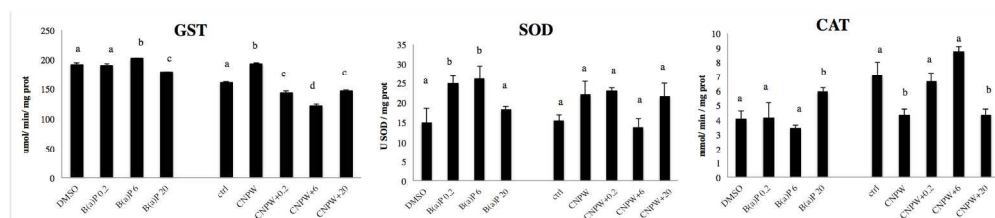
209x297mm (300 x 300 DPI)



Modulation of genes (*cyp1a*, *hsp70*, *sod1*, *sod2*) in zebrafish embryos (96 hpf) exposed to CNPW (50 mg/L) and B(α)P (0.2, 6, 20 μg/L) alone and in combination. Results are expressed as fold induction over control (ZFW or DMSO for CNPW alone and contaminated or B(α)P respectively) (± SEM). 18S is used as housekeeping gene. The threshold for biological significance  $0.5 < > 2$  is pointed out.

218x182mm (150 x 150 DPI)

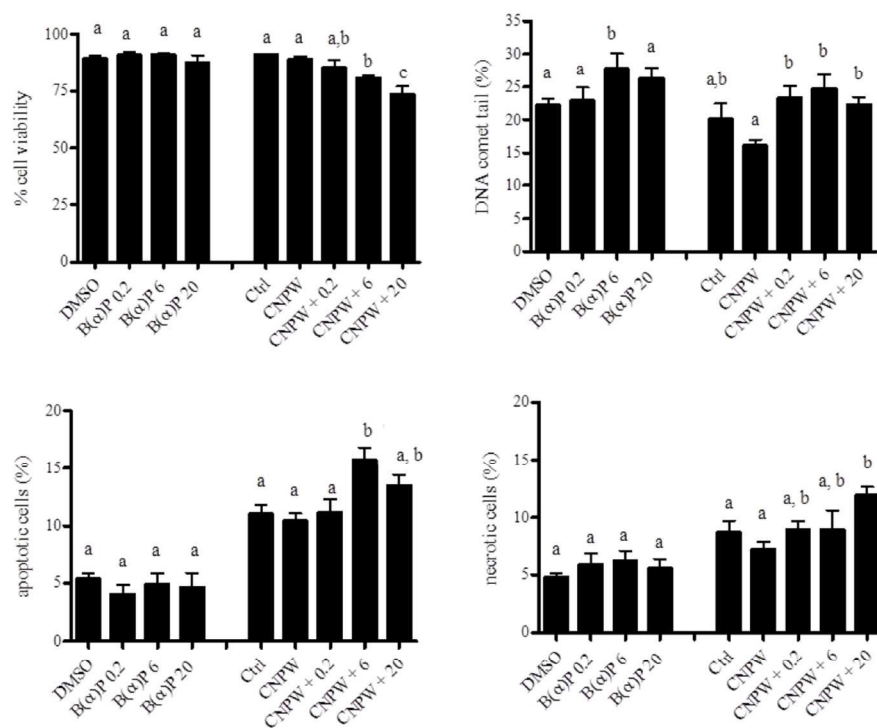
 1  
2  
3  
4  
5  
6  
7  
8  
9  
10  
11  
12  
13  
14  
15  
16  
17  
18  
19  
20  
21  
22  
23  
24  
25  
26  
27  
28  
29  
30  
31  
32  
33  
34  
35  
36  
37  
38  
39  
40  
41  
42  
43  
44  
45  
46  
47  
48  
49  
50  
51  
52  
53  
54  
55  
56  
57  
58  
59  
60



Effects of CNPW (50 mg/L) and B(a)P (0.2, 6, 20  $\mu$ g/L) alone and in combination on the activity (mean  $\pm$  SEM) of glutathione S-transferase (GST); catalase (CAT) and superoxide dismutase (SOD) measured in zebrafish embryos (96 hpf) (n = 3; pool of 3 independent experiments). Different letters indicate significantly different values (one-way ANOVA, Fischer's LSD post hoc test, p < 0.05).

254x58mm (300 x 300 DPI)

 1  
2  
3  
4  
5  
6  
7  
8  
9  
10  
11  
12  
13  
14  
15  
16  
17  
18  
19  
20  
21  
22  
23  
24  
25  
26  
27  
28  
29  
30  
31  
32  
33  
34  
35  
36  
37  
38  
39  
40  
41  
42  
43  
44  
45  
46  
47  
48  
49  
50  
51  
52  
53  
54  
55  
56  
57  
58  
59  
60



Cyto-genotoxic effects of CNPW (50 mg/L) and B(a)P (0.2, 6, 20 µg/L) alone and in combination, measured as mean ( $\pm$  SEM) cell viability, DNA strand breaks and occurrence of apoptotic and necrotic cells in zebrafish embryos (96 hpf) ( $n = 3$ ; pool of 3 independent experiments). Different letters indicate significantly different values (one-way ANOVA, Fischer's LSD post hoc test;  $p < 0.05$ ).

209x163mm (150 x 150 DPI)

 1  
2  
3  
4  
5  
6  
7  
8  
9  
10  
11  
12  
13  
14  
15  
16  
17  
18  
19  
20  
21  
22  
23  
24  
25  
26  
27  
28  
29  
30  
31  
32  
33  
34  
35  
36  
37  
38  
39  
40  
41  
42  
43  
44  
45  
46  
47  
48  
49  
50  
51  
52  
53  
54  
55  
56  
57  
58  
59  
60